Riad Bouzidi [1], Ismail Ghadbane[1], Mohammed Boukhari[1]

Electrical Engineering Laboratory, Department of Electrical Engineering, University of Msila, Algeria (1)

doi:10.15199/48.2022.11.02

Experimental Study of an Induction Motor Using Scalar Control Method Applied in Electric Vehicle

***Abstract**. This paper present the scalar control method applied in an electric vehicle, witch use an induction motor for its drive, where the dSPACE MicroLabBox is used as a real time interface (RTI) for SIMULINK. At first we present the induction motor model in the dqo axis, and the control method, then we present the dynamic model of the vehicle. Finally, the figures show materials used, and the experimental results obtained by experiment software Control Desk.*

***Streszczenie.** W artykule przedstawiono metodę sterowania skalarnego zastosowaną w pojeździe elektrycznym wykorzystującym do napędu silnik indukcyjny, gdzie dSPACE MicroLabBox jest używany jako interfejs czasu rzeczywistego (RTI) dla SIMULINK. Najpierw przedstawiamy model silnika indukcyjnego w osi dqo oraz sposób sterowania, następnie przedstawiamy model dynamiczny pojazdu. Wreszcie, rysunki przedstawiają użyte materiały i wyniki eksperymentalne uzyskane za pomocą oprogramowania doświadczalnego Control Desk. (**Badanie eksperymentalne silnika indukcyjnego z wykorzystaniem metody sterowania skalarnego stosowanego w pojeździe elektrycznym**)*

Keywords: Electric Vehicle (EV), induction motor (IM), scalar control, dSPACE MicroLabBox, Control Desk.
Słowa kluczowe: Pojazd elektryczny, silnik indukcyjny, kontrola skalarna, dSPACE MicroLabBox, Panel sterowania.

Introduction

The electric car is one of the most environmentally friendly modern technologies to day, where it does not emit harmful fumes, and it depends on electricity (batteries) as a source of energy. Unlike the conventional internal combustion vehicle, which in turn leaves toxic gases harmful to the living environment and also depends on fossil fuels as a source of energy .

An electric car compensates the human better than the conventional internal combustion vehicle, that is why many studies today focus on this aspect of technology (electric car), as studies differ in all areas related to the electric vehicle, according to the diversity of its parts. One of the most principal part of the electric vehicle is the motor, where we have many types of it, such us the induction motor IM, the direct current motor DCM, the switched reluctance motor SRM and the interior permanent synchronous motor IPM, each of these motors has its own control structure, advantages and disadvantages, we choose the appropriate motor according to the type, cost, power and size of the vehicle[1].

In our study, we choose the induction motor, due to its availability, simple and robust construction. The major advantage of induction motors is that they are powerful and can operate in any environmental conditions, also are cheaper due to the absence of brushes, commutators and slip rings. There are three basic methods of induction motor control, which are scalar control, field oriented control (FOC) and direct torque control (DTC)[2]- [6].

Several scalar controls exist depending on whether one acts on the current or on the voltage. They depend above all on the topology of the converter (voltage inverter or current). The voltage inverter being now the most used in small and medium power, it is the V/f control the most used. In this study, we choose to control the induction motor with (v/f control), as it is simple and low cost control, compared to the other two controls (FOC and DTC), the principle of scalar control is to maintain the value of the voltage on frequency constant (V/f = constant), which means to keep the flux constant, so the torque is controlled by the action on the slip[3]. However, to obtain this control we need to have the instantaneous value of the motor speed, in this case, we use the speed sensor (encoder). We use dSPACE MicroLabBox as a communication medium to know the motor speed value and give the inverter gates signals. Fig. 1 Shows the induction motor control schema.

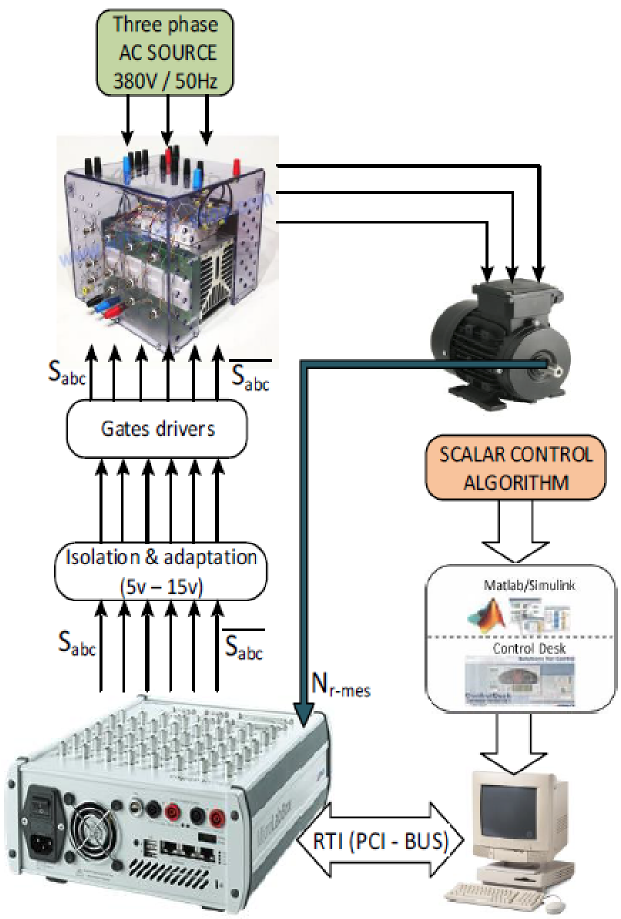

Fig. 1. Basic scalar control schema.

The induction motor model

Fig.2 Shows the equivalent circuit of the induction motor, where the model is in the dqo axis [4], and according to this circuit, we can write the mathematical model of the induction motor as:[7]

(1) $$[\dot{I}]=[L]^{-1}\{[V]-[R][I]\}$$

such as:

$$[I]=\begin{bmatrix} i_{ds} \\ i_{qs} \\ i_{dr} \\ i_{qr} \end{bmatrix};[V]=\begin{bmatrix} v_{ds} \\ v_{qs} \\ v_{dr} \\ v_{qr} \end{bmatrix};[L]=\begin{bmatrix} L_s & 0 & M & 0 \\ 0 & L_s & 0 & M \\ M & 0 & L_r & 0 \\ 0 & M & 0 & L_r \end{bmatrix}$$

$$[R]=\begin{bmatrix} R_s & -\omega_s L_s & 0 & -\omega_s M \\ \omega_s L_s & R_s & \omega_s M & 0 \\ 0 & -\omega_{sl} M & R_r & -\omega_{sl} L_r \\ -\omega_{sl} M & 0 & \omega_{sl} L_r & R_r \end{bmatrix}$$

where d and q are the dqo axis. i; is the current. v; is the voltage. R; is the resistance. L is the inductance. M; is the magnetizing inductance. ω; is the angular speed. ω_{sl}; is the slip speed. s and r represent the stator and the rotor. The flux equations can be expressed as:

(2) $$[\Phi]=[L][I]$$

such as:

$$[\Phi]=\lfloor \Phi_{ds} \quad \Phi_{qs} \quad \Phi_{dr} \quad \Phi_{qr} \rfloor^T$$

where Φ represent the magnetic flux.

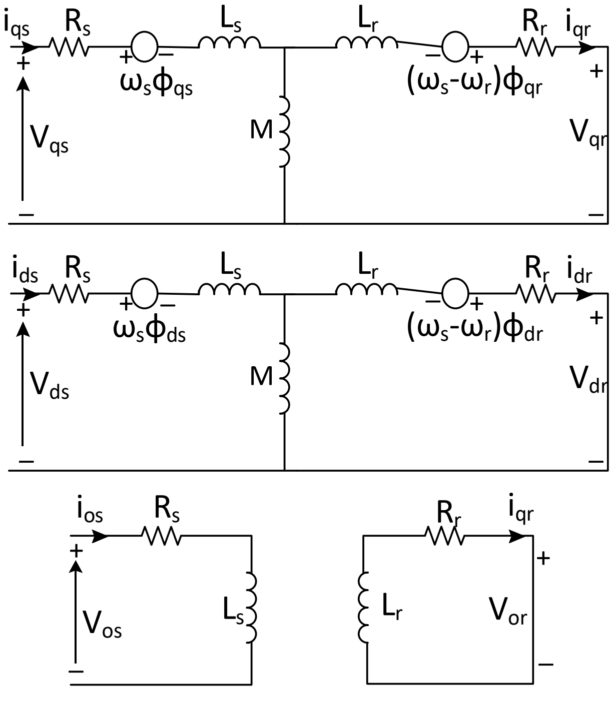

Fig. 2. Equivalent circuit of induction motor in dqo axis

The electromagnetic torque and speed can be expressed as :

(3) $$T_e=\frac{3}{2}p\frac{M}{L_r}(i_{dr}i_{qs}-i_{ds}i_{qr})$$

(4) $$\Omega_r=(T_e-T_r)\frac{1}{J.S+C_f}$$

such as: T_e is the electromagnetic torque. p is the number of pole pairs. Ω_r is the rotor speed. T_r is the load torque. J is the moment of inertia. C_f is the friction coefficient. S is the Laplace operator.

Scalar control algorithm

The scheme shown in the Fig.4; represent the block scalar control control algorithm in Fig.1, the regulator is of type *PI*; where through the speed error, it can give us the value of the reference slip speed $\omega_{sl}*$ as the equation below [8]:

(5) $$\omega_{sl}^{*}=(\omega_r^{*}-\omega_{r_{mes}})\times(k_p+\frac{k_i}{S})$$

where: ω_r^* and ω_{rmes} are the reference and measured speed respectively. k_p and k_i are the proportional and integral gain of the PI regulator respectively, and we can get their values through the following[3]:

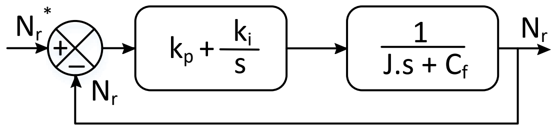

Fig. 3. Speed regulation.

According to the Fig.3; we can determine the open loop transfer function T_{oL} as follows:

(6) $$T_{oL}=\frac{N_r}{N_r^{*}}=\frac{k_p.S+k_i}{J.S^2+C_f.S}$$

The closed loop transfer function T_{cL} is obtained by the following equation:

(7) $$T_{cL}=\frac{T_{oL}}{1+T_{oL}}=\frac{\dfrac{k_p.S+k_i}{J}}{S^2+\dfrac{k_p+C_f}{J}.S+\dfrac{k_i}{J}}$$

The canonical form of a second order transfer function T_{cf} is given by:

(8) $$T_{cf}=\frac{k}{S^2+2\xi\omega_n.S+\omega_n^{2}}$$

when ξ represents the damping coefficient and ω_n is the own pulse. Matching T_{cL} with T_{cf}, we find:

(9) $$k_p=2\xi\omega_n J-C_f$$
$$k_i=\omega_n^{2}J$$

After the calculation we find: $k_p = 0.025$; $k_i = 0.001$

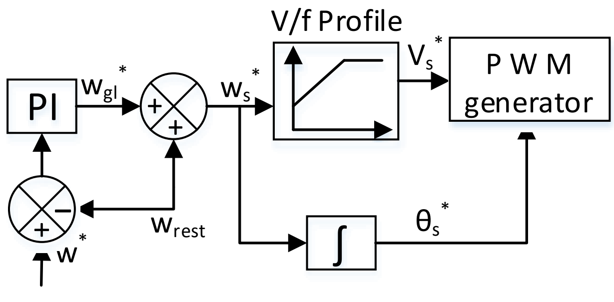

Fig. 4. Scalar control block.

We get the stator reference speed pulsation ω_s^* with the following equation:

$$\omega_s^* = \omega_{r_{mes}} + \omega_{sl}^* \tag{10}$$

In the following equation we note that the voltage V_s is the same whatever is the reference considered[7].

$$\overline{V_s} = R_s \overline{I_s} + j\omega_s \overline{\Phi_s} \tag{11}$$

To keep the flux constant, the voltage V_s efficiency must be proportional to the supply frequency of the stator f_s , at high speed R_sI_s is too small compared to ω_s, so we can write as follows :

$$\Phi_s = \frac{V_s}{\omega_s} = \frac{V_s}{2\pi f_s} \tag{12}$$

However, this relation is not valid for low value of the pulsation ω_s, because the voltage drop R_sI_s due to the resistance of the stator windings is no longer negligible compared to the term $\omega_s\Phi_s$ [9]

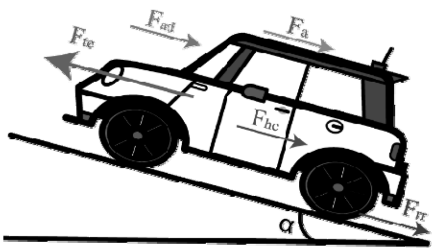

Fig. 5. Types of forces applied to the vehicle.

vehicle dynamic model

In order to study vehicle control, it is necessary to have a model which accounts for the dynamic of the vehicle from the tensile forces developed by its actuators and the resistance forces to displacement. Fig.5 Shows the different forces applied to the vehicle [8]. Where each of these forces has its own relation, and can be written as follows:

$$F_{ad} = \frac{1}{2}\rho C_d A V^2 \tag{13}$$

where F_{ad} is the aerodynamic drag force. ρ is the air density. C_d the drag coefficient. A is the surface of vehicle (windward area) and V is the velocity.

$$F_{rr} = K_r m g \tag{14}$$

where F_{rr} is the rolling resistance force. K_r is the tire rolling resistance coefficient. m is the total mass of the vehicle and g is the gravity acceleration.

$$F_{hc} = mg\sin(\alpha) \tag{15}$$

where F_{hc} is the hill climbing force, and α is the road slop angle.

$$\begin{aligned} F_a &= M_e a \\ M_e &= 1.04 + 0.0025 g_r^2 \end{aligned} \tag{16}$$

where F_a is the acceleration force. a is the vehicle acceleration and g_r is the gear ratio [9].

$$F_{te} = \sum F = F_{ad} + F_{rr} + F_{hc} + F_a \tag{17}$$

where F_{te} is the total traction effort. The power of the motor P_m and the torque load applied from the vehicle to motor T_{rr} are given by:

$$\begin{aligned} P_m &= \frac{1}{\eta} F_{te}.V \\ T_{rr} &= (F_{ad} + F_{rr} + F_{hc}) \frac{R}{g_r} \end{aligned} \tag{18}$$

where, R is the weal radius, and η is the motor efficiency.

Experimental results

The test bench shown in Fig.6, present the material utilize in our experiment, where in addition to the induction motor, we have an inverter type SEMIKRON; witch is attacked by the gates drive in his IGBT interrupter, then he gives the appropriates voltages to the motor according to the gates pulsations, speed sensor (encoder); to measure the instantaneous value of the motor speed, the whole control algorithm witch is in MATLAB/SIMULINK and the measured speed are implemented in dSPACE MicroLabBox within $50\mu s$ to generate digital control signals via PWM outputs; where the control frequency is about 10KHz, the magnetic powder break is used to generate the resistance torque T_r where is applied to the motor in load test.

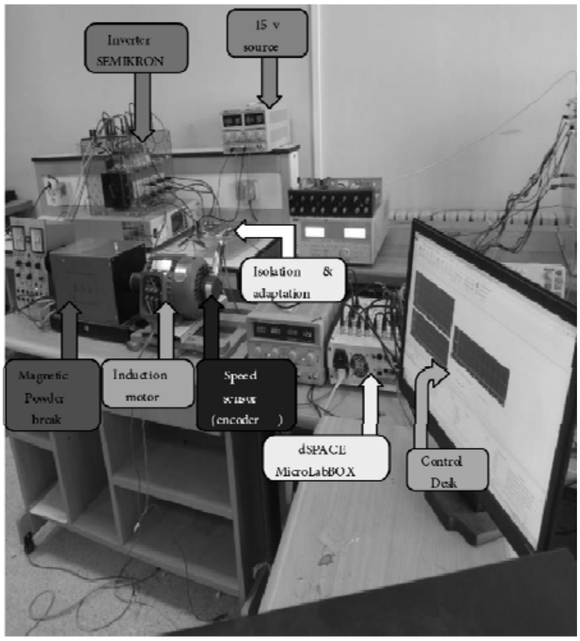

Fig. 6. Experiment prototype for laboratory

fixed reference test)

Where we have fixed the reference speed value N_r^* at $1200 rpm$, Fig.7 shows the results of this test.

different speed test)

In this case, we test the motor robustness by applying different values of the reference speed N_r^*, where the expermental results are in Fig.8.

reverse speed test

This test is for reversing the motor direction, where the results are in Fig.9.

load test

This test is for fixing the reference speed value (N_r^*) at $1200 rpm$ and applying a load torque $T_r = 2N.m$ at $t = 44s$, the results are shown in Fig.10.

scenario load test

In this case, we applied an scenario of the load torque as shown in Fig.11(a),and fixing the reference speed value (N_r^*) at $1200 rpm$, the results are shown in Fig.11.

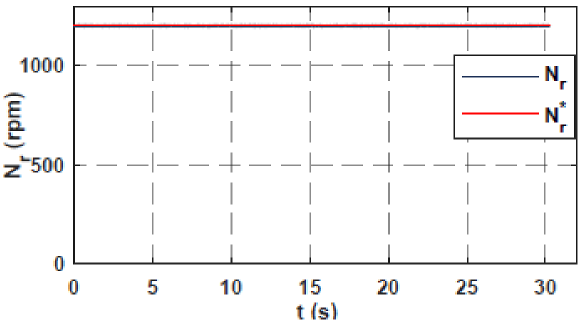

(a) The motor speed N_r

(b)

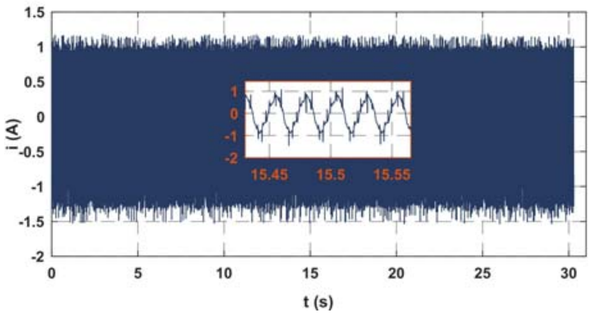

b - The current (i)

Fig. 7. fixed reference test

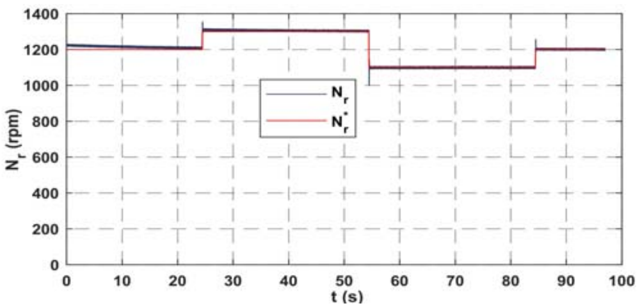

(a) The motor speed N_r

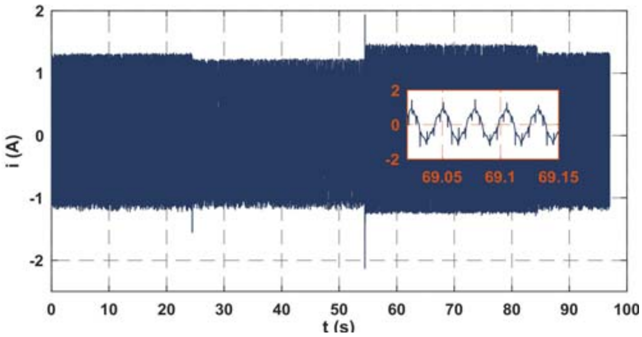

b - The current (i)

Fig. 8. Different speed test

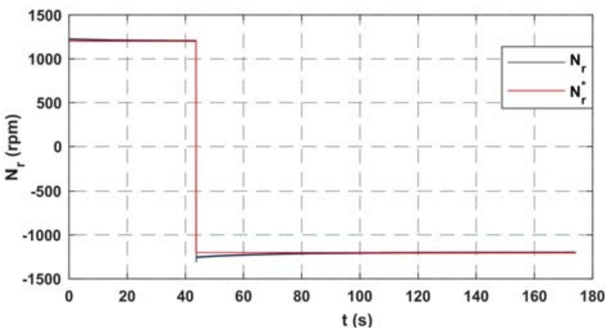

(a) The motor speed N_r

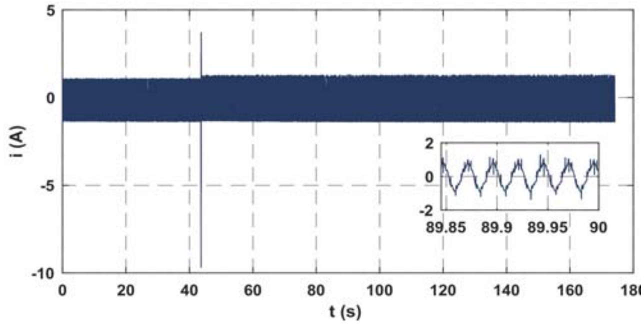

(b) The current (i)

Fig. 9. reverse speed test

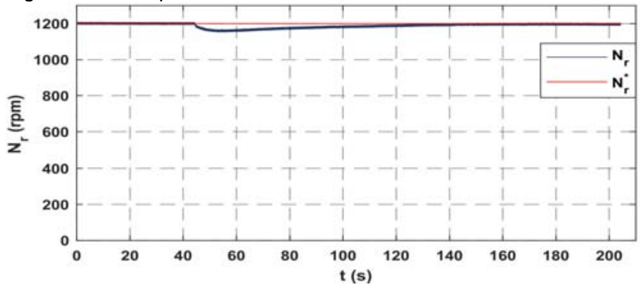

(a) The motor speed N_r

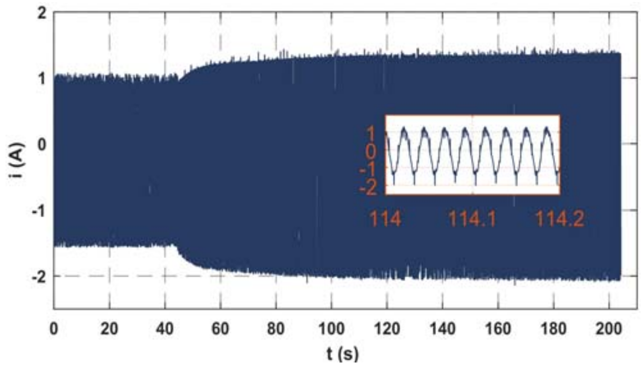

b) The current (i)

Fig. 10. Torque load test

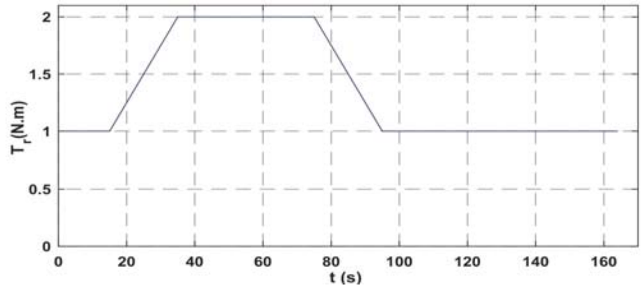

(a) Load torque profile T_r

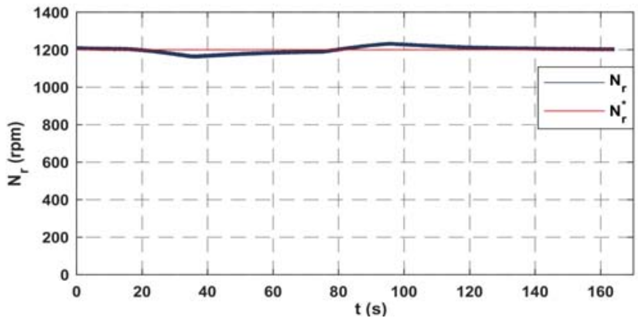

(b) The motor speed N_r

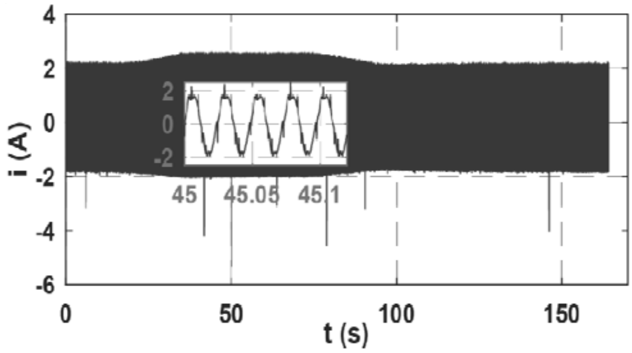

c) The current (i)

Fig. 11. Scenario load test

Conclusion

This paper has presented an experiment (v/f) control of an induction motor drives used in electric vehicle, where the vehicle dynamic model was presented as the torque load on the motor. Several tests were conducted to the motor and according to its performance we can say that this control method gave us acceptable results, knowing that we used one speed sensor to regulate the speed, unlike the other technique of control (FOC, DTC) they use more than that. The experiment results with all the tests has been verified that this control method strategy is allowed to apply in an electric vehicle motor drive.

Table 1. The induction motor parameters

Induction motor	Unit	Value
P_n	kw	0.55
V_n	V	230/400
i_n	A	2.48/1.43
N_n	rpm	1390
f	Hz	50

Authors: *Dr .Bouzidi riad, LGE laboratory ,Faculty of technology , M'sila University, Algeria.Email : riad.bouzidi@univ-msila.dz*
Dr. IsmailGhadbane , LGE laboratory ,Faculty of technology , M'sila University, Algeria.Email : ismail.ghadbane@univ-msila.dz
Boukhari Mohamed, LGE laboratory Phd student at Department of Electrical Engineering ,Faculty of technology , M'sila University, Algeria. Email: mohammed.boukhari@univ-msila.dz

REFERENCES

[1] M. Ehsani, K. V. Singh, H. O. Bansal, and R. T. Mehrjardi, "State of the Art and Trends in Electric and Hybrid Electric Vehicles," *in Proceedings of the IEEE, vol. 109, no. 6, pp. 967-984, June 2021,* doi: 10.1109/JPROC.2021.3072788.
[2] C. C. Chan and Y. S. Wong, "The state of the art of electric vehicles technology," in *Proc. 4th IPEMC*, 2004, vol. 1, pp. 46–57.
[3] C. C. Chan, "The state of the art of electric and hybrid vehicles," *Proc. IEEE*, vol. 90, no. 2, pp. 247–275, Feb. 2002.
[4] L. Situ, "Electric vehicle development: The past, present and future," in Proc. 3rd Int. Conf. PESA, 2009, pp. 1–3.
[5] Mbadiwe, Enwelum I., et al. "Permanent magnet flux switching motor technology as a solution for high torque clean electric vehicle drive." *International Journal of Power Electronics and Drive System (IJPEDS)* 10.2 (2019): 575-584.
[6] ZIA, Akif. A comprehensive overview on the architecture of hybrid electric vehicles (hev). *In : 2016 19th International MultiTopic Conference (INMIC). IEEE, 2016*. p. 1-7.
[7] CHAU, Kwok Tong. Electric vehicle machines and drives: design, analysis and application. John Wiley & Sons, 2015.
[8] YU, Jianfeng, ZHANG, Ting, et QIAN, Jianming. Electrical motor products: *International energy-efficiency standards and testing methods.* Elsevier, 2011.
[9] RAI, Tripti et DEBRE, Prashant. Generalized modeling model of three phase induction motor. In : *2016 International Conference on Energy Efficient Technologies for Sustainability (ICEETS). IEEE*, 2016. p. 927-931.
[10] CHEN, Frank et CHEUNG, Richard. Advanced Speedsensorless Induction-motor Drive. In : 2007 *Large Engineering Systems Conference on Power Engineering. IEEE*, 2007.p. 265-269.
[11] SMITH, Andrew, GADOUE, Shady, ARMSTRONG, Matthew, et al. Improved method for the scalar control of induction motor drives. *IET electric power applications*, 2013, vol. 7, no 6, p. 487-498.
[12] TRZYNADLOWSKI, Andrzej M. Control of induction motors. Elsevier, 2000.
[13] SAIDI, Hemza, TALEB, Rachid, MANSOUR, Noureddine, et al. Three phase inverter using SVPWM method for solar electric vehicle. In : IREC2015 *The Sixth International Renewable Energy Congress*. IEEE, 2015. p. 1-5.
[14] HADDOUN, Abdelhakim, BENBOUZID, Mohamed El Hachemi, DIALLO, Demba, et al. A loss-minimization DTC scheme for EV induction motors. *IEEE Transactions on vehicular technology*, 2007, vol. 56, no 1, p. 81-88